Colloid Polym Sci (2002) 280: 963–967
DOI 10.1007/s00396-002-0706-z

ORIGINAL CONTRIBUTION

Sung-Woo Park
Jin-Woong Kim
Jung-Bae Jun
Kyung-Do Suh

Nanostructured latex films from poly(butyl methacrylate) latex cross-linked with poly (ethylene oxide)–poly(propylene oxide)–poly(ethylene oxide) triblock macro-cross-linker

Received: 25 October 2001
Accepted: 27 March 2002

S.-W. Park · J.-B. Jun · K.-D. Suh (✉)
Division of Chemical Engineering,
College of Engineering,
Hanyang University, Seoul 133-791, Korea
E-mail: kdsuh@hanyang.ac.kr
Tel.: +82-2-22900526
Fax: +82-2-22952102

J.-W. Kim
Cosmetics Research Institute, Pacific
Corporation R&D Center, 314-1 Bora-ri,
Kiheung-eup, Yongin-si, Kyunggi-do,
449-900, Korea

Abstract Biphasic polymer latexes were synthesized by a seeded swelling and polymerization method. The latexes were composed of a poly(butyl methacrylate) core and a poly(ethylene oxide) rich shell cross-linked with poly(ethylene oxide)-poly (propylene oxide)–poly(ethylene oxide) triblock diol diacrylate macro-cross-linker. Nanostructured films were obtained by annealing the biphasic polymer latexes at a temperature between the glass-transition temperatures of the core latex and the cross-linked poly(ethylene oxide) based shell. Atomic force microscope images of the latex film revealed that the poly(butyl methacrylate) core phase is confined in the poly(ethylene oxide)-rich continuous phase with the form of separate nanosized spheres.

Keywords Triblock macro-cross-linker · Biphasic polymer latex · Nanostructured latex film · Atomic force microscope image

Introduction

Polymer latex films find a great number of applications in the fields of paints, coatings, textiles, papers, and adhesives [1, 2]. Although many researchers still propose somewhat different mechanisms to account for the formation of polymer latex films, a generally acceptable one can be summarized with three steps [2, 3, 4]: a linear cumulative water loss and an irreversible contact between particles; a deformation of the particles and a close contact between the particles by means of large interfacial forces; and the diffusion of polymer chains through the contact surfaces (autohesion). In this process, one should consider the glass-transition temperature, T_g, [5, 6] and cross-linking [3, 7, 8] of the latex polymers, the water resistance [9], the presence of surfactants [10, 11], and so on. Until now most studies have dealt with theoretical or, in some aspects, the basic experimental approach of the formation of homopolymer latex films, except for the consideration of the effect of additives such as surfactants. For the past decade, however, some research groups have studied the film formation of core–shell latex particles [12, 13, 14]. Nevertheless, there are only a few reports of investigations of structured polymer latex films; these investigations are needed to improve the inherently poor mechanical properties of conventional latex films and to introduce high functional moieties to the film phase. There also have been no studies to investigate the film formation of shell–cross-linked polymer latexes.

In this study, we present nanostructured polymer latex films that are synthesized by considering systematically the morphology of the latex phases. To synthesize tailor-made biphasic polymer latexes, the latex structure was designed with a polymer core and a cross-linked poly(ethylene oxide)-rich shell. The film-forming process of such latexes can be significantly affected by the triblock macro-cross-linker surrounding the poly(butyl methacrylate) (PBMA) core particles. Besides, the functionality of the film formed from such composite latexes is governed by the characteristics of the shell.

Experimental

Materials

Poly(ethylene oxide)–poly(propylene oxide)–poly(ethylene oxide) (PEO–PPO–PEO) triblock diol (t-BD, $M_w = 1.1\times10^3$, 2.0×10^3, 2.8×10^3 gmol^{-1}, Aldrich Chemical Co.) was dried under vacuum at 80 °C for 3 h. Acrylolyl chloride (AC, Acros Organics), triethylamine (TEA, Aldrich), and potassium persulfate (KPS, Aldrich) were of reagent grade. The inhibitor in *n*-butyl methacrylate (BMA, Aldrich) was removed using a removing column (Aldrich).

Synthesis of triblock diol diacrylate

Triblock diol diacrylate (t-BDDA) (Scheme 1) was synthesized by the reaction of t-BD with AC. t-BD (1 mol) dissolved in tetrahydrofuran was poured in a 500-ml round-bottomed flask and cooled to 0 °C. TEA (2 mol) and AC (2 mol) were added into the flask and reacted at 70 °C for 5 h under vigorous stirring. Then, the reaction mixture was filtered to remove the salt and triethanolamine hydrochloride, and evaporated completely. Continuously, remnant salts and unreacted starting material were removed by washing with a methylene chloride/water mixture. After trapping the moisture, the solution was evaporated until a viscous liquid was recovered.

Preparation of latex and characterizations

Surfactant-free PBMA seed latex was produced by batch-free radical emulsion polymerization. KPS (0.3 g) and water (170 g) were weighed into a four-necked round flask equipped with a reflux condenser, a nitrogen inlet apparatus, and a mechanical stirrer. Under a nitrogen atmosphere, the reactor was submerged in a thermostated water bath and the mixture was stirred with a rotation speed of 250 rpm at 75 °C. After 10 min, *n*-BMA (30 g) was added to the reactor and polymerized for 6 h. Continuously, the preformed PBMA seed latex was swollen uniformly with a monomer mixture (30 g) emulsified finely in water (120 g) by ultrasonic homogenization. The monomer mixture was composed of *n*-BMA, t-BDDA (0–15 mmol) and benzoyl peroxide (0.3 g, Aldrich). The swelling was continued with gentle stirring at 5 °C for 10 h. After deaerating with nitrogen gas, the polymerization was carried out at 70 °C for 6 h.

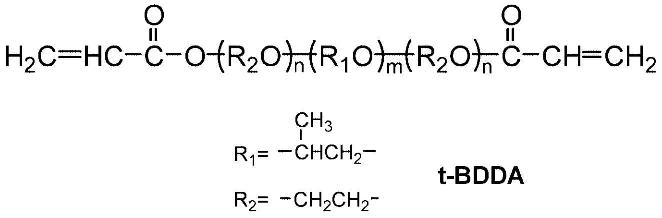

$H_2C{=}HC{-}\overset{O}{\overset{\|}{C}}{-}O{\leftarrow}(R_2O)_n(R_1O)_m(R_2O)_n{-}\overset{O}{\overset{\|}{C}}{-}CH{=}CH_2$

$R_1 = -CH(CH_3)CH_2-$

$R_2 = -CH_2CH_2-$

Scheme 1. Structure of triblock diol diacrylate (*t-BDDA*)

Latex films were prepared by casting one drop of the latex dispersions onto a square plate of well-polished mica of side of about 10 mm and each drop was allowed to air-dry at 20 °C for 3 h. The topography of the latex films was observed using a Nanoscope III atomic force microscope (AFM) from Digital Instruments, operated in the tapping mode. The tip was silicon with a spring constant of 50 N/m and the cantilever oscillated at its proper frequency (about 350 kHz). To determine the structure and relaxation of the PBMA/t-BDDA latex films, the dielectric properties of the latex films were measured, by scanning the temperature, at a selected frequency of 1 Hz with a dielectric analyzer (DEA, TA Instruments). The tensile properties of the latex films were determined using an Instron universal tensile testing machine at room temperature. Standard tensile test specimens were cut from the latex films using a metallic die. A 500-N load cell was employed, and the experiments were run at a crosshead speed of 25 mm/min.

Results and discussion

The biphasic latex was synthesized by a seeded swelling and polymerization method. For an effective diffusion of monomers into the seed particles, the monomer mixture should be added in the form of a fine emulsion [15]. It is important to realize that the t-BDDA has a pronounced surface activity at low temperature owing to its hydrophilic/hydrophobic/hydrophilic molecule chain and phase behavior [16]. The t-BDDA used in this study had a lower critical solution temperature in water, around 15 °C, at a concentration of 0.1–3wt% (Table 1). Therefore, at low temperature, t-BDDA is very effective in emulsifying the monomers in water, helping significantly the diffusion of monomer droplets into the seed latex. After complete swelling of the monomer mixture

Table 1. Characteristics of the polymer latexes and their films. In the case using triblock diol diacrylate (*t-BDDA*), its concentration was fixed at 10 mmol. Poly(butyl methacrylate): *PBMA*

Latex	t-BDDA			D_n (nm)[b]	Root mean square (nm)[c]
	M_n ($\times10^3$ gmol^{-1})	M_w/M_n	T_c[a]		
PBMA	–	–	–	591 ± 8	33.18
PBMA/t-BDDA1	1.19	1.10	15.0	582 ± 4	25.71
PBMA/t-BDDA2	2.11	1.09	16.0	563 ± 6	26.22, 18.23 (Fig. 1c-1)
PBMA/t-BDDA3	3.01	1.18	15.5	564 ± 5	17.39

[a] Cloud point measured with a thermooptical microscope at 0.5 wt% t-BDDA concentration in water

[b] Diameters of final latexes measured with an electrophoretic light scattering particle analyzer (ELS-800, Photal Otsuka Electronics)

[c] Surface roughness obtained from the Nanoscope III software, as follows:

$$(\text{Root mean square})^2 = \frac{1}{n}\sum_{1}^{n}[z(i) - z_0]^2, \quad z_0 = \frac{1}{n}\sum_{1}^{n} z(i),$$

where n is the number of z values used and $z(i)$ is the height of point i

emulsions, the polymerization resulted in a highly monodisperse latex having the morphology of a PBMA core and a cross-linked PEO-rich soft shell.

AFM images of PBMA/t-BDDA2 latex films synthesized by changing the concentration of t-BDDA are shown in Fig. 1. On increasing the concentration of t-BDDA, space-filling polyhedra started to appear and the surface of the films was gradually flattened (the root-mean-square, rms, value was reduced from 33.18 to 22.96 nm). At 15 mmol t-BDDA, the film exhibited a honeycomb-like structure. Considering the drying temperature of 20 °C, which is located between the T_g of the PBMA core (24 °C) and the PEO-rich shell (below 0 °C), it is clear from these results that the soft shells touch each other through the contact surfaces and particle deformation takes place readily as the water in the interstitial space evaporates. Even when the film was annealed sufficiently at 50 °C, the uniformly phase separated film morphology and spherical cap structure were observed, as shown in Fig. 1c-1. In addition, the surface roughness was reduced dramatically with an rms value of 18.23 nm (Table 1). With reference to the topology shown in Fig. 1c-1, it is reasonable to think that only PEO-rich phases were mixed selectively through the contact surfaces by the chain migration between adjacent particles and the phase mixing between the PBMA core and the PEO-rich shell did not happen even at an annealing temperature higher than the T_g of PBMA. In this system, because the shell phase is cross-linked by t-BDDA and the cross-linked PEO-rich shell has quite limited miscibility with the PBMA core [10], polymer diffusion can occur preferentially across the intercellular boundary between the cross-linked PEO-rich shell phases of the adjoining particles [8]. Therefore, this limited interdiffusion resulted in a structured film morphology, in which the PBMA phase is confined in the PEO-rich continuous phase with the form of nanosized spherical caps.

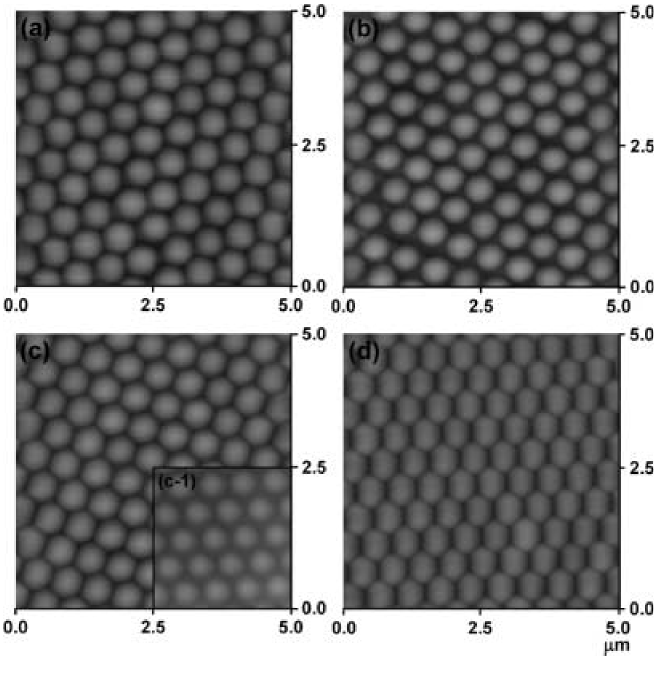

Fig. 1. Atomic force microscope (*AFM*) images of poly(butyl methacrylate) (*PBMA*)/triblock diol diacrylate (*t-BDDA2*) latex films annealed at 20 °C for 3 h by varying the concentration of t-BDDA2 in the second monomer mixtures: **a** 0 mmol, **b** 5 mmol, **c** 10 mmol, and **d** 15 mmol. The AFM image **c-1**, represented separately in **c**, is the PBMA/t-BDDA2 latex film annealed fully at 50 °C for 12 h at the same composition as that in **c**

The effect of the molecular weight of t-BDDA on the film topology was observed at the same concentration of t-BDDA and is shown in Fig. 2. The honeycomb structure was more pronounced at higher molecular weights of t-BDDA. The latex film containing 10 mmol t-BDDA3 also displayed the spherical-cap structure and very smooth surface roughness (rms = 17.39 nm), even if dried at a temperature of 20 °C. The lower degree of cross-linking of the PEO-rich shell seems to allow not only the effective migration of network chains between adjacent particles, but also a distinct phase separation between the PBMA core and the PEO-based shell. Farinha and Martinho [17] demonstrated that surface PEO chains grafted in the PBMA polymer promote mixing and interdiffusion during the drying process and the shorter free PEO chains added separately diffuse quickly at short annealing times. In our system, how-

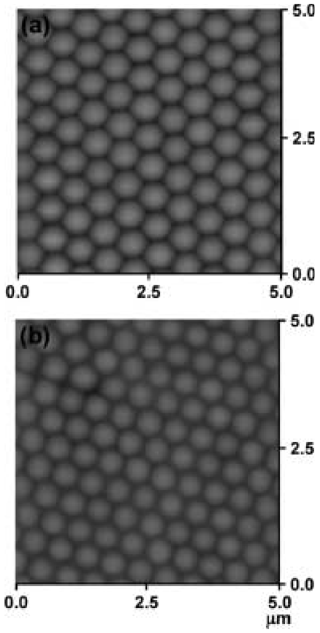

Fig. 2. AFM images of PBMA/t-BDDA latex films annealed at 20 °C for 3 h by varying the molecular weight of t-BDDA: **a** t-BDDA1 and **b** t-BDDA3. The concentration of t-BDDA in the second monomer mixtures was fixed at 10 mmol

ever, it is believed that polymer chains cross-linked with longer PEO–PPO–PEO chains (with higher molecular weight) can diffuse more readily at the contact surfaces owing to their higher mobility.

The dielectric properties of PBMA/t-BDDA latex films were measured with a DEA and are shown in Fig. 3. The PBMA homopolymer latex film showed only one transition, at 24 °C. In contrast, the PBMA/t-BDDA latex film showed two transitions, at –58 and 24 °C, respectively. This result confirms that the latex film is composed of two distinct phases of PBMA (cap region) and PEO (continuous region).

The mechanical properties of the PBMA/t-BDDA and PBMA/t-BD latex films are shown in Fig. 4. To examine the effect of cross-linking on the mechanical properties of the latex films, PBMA/t-BD latex film was produced by replacing t-BDDA of the monomer mixture added into the seed latex with t-BD2. As the molecular weight of t-BDDA cross-linker increased, the tensile strength of the latex films increased steeply; on the other hand, the tensile elongation decreased slightly. At equimolar concentration of cross-linkers, a long-chain cross-linker could give large polymer networks of the particles, allowing the enhancement of chain mobility, which is an important factor for the interparticle chain diffusion. Moreover, the tensile strength of the PBMA/t-BDDA2 latex film increased by about 59% compared to that of the PBMA/t-BD latex film, but the elongation of the cross-linked latex film was about 24% lower than that of the PBMA/t-BD latex film. The contrast between the mechanical behavior of the two latex films can be explained by the difference in the existence of cross-linking and the degree of interparticle diffusion [8, 18]. The cross-linking by t-BDDA was expected to enhance the chain stiffness, and resulted in higher tensile strength. However, the decrease in the elongation of the PBMA/t-BDDA latex films can be attributed to the slower diffusion rate and the lower mass fraction of mixing caused by the network structure interfering with the chain diffusion.

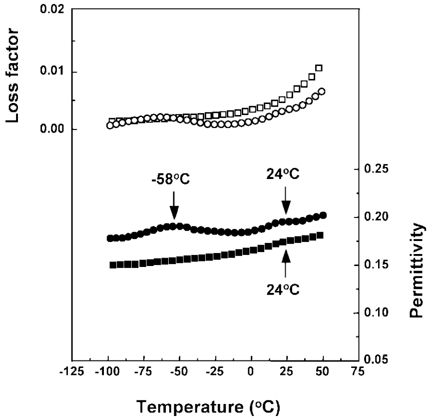

Fig. 3. Dielectric analyzer diagrams of the latex films annealed fully at 50 °C for 3 days before the measurements: Loss factor (*open symbols*) and permittivity (*closed symbols*) for PBMA homopolymer latex film (*squares*) and PBMA/t-BDDA2 latex film containing 10 mmol t-BDDA (*circles*)

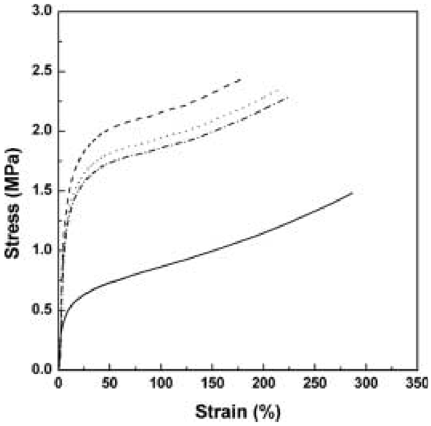

Fig. 4. Stress–strain curves for PBMA latex films containing different diol-based molecules: triblock diol (*t-BD2*) (–), t-BDDA1 (– –), t-BDDA2 (·····), and t-BDDA3 (–·–). The latex films were annealed fully at 50 °C for 3 days before measurement and the concentration of t-BDDA and t-BD2 in the second monomer mixtures was fixed at 10 mmol

Conclusion

t-BDDA was very effective in the diffusion of monomer droplets into the seed latex at low temperature. After the polymerization, the polymer latex was expected to have the morphology of a PBMA core and a cross-linked PEO-based soft shell. In reality, the latex films prepared from the biphasic polymer latexes exhibited a space-filling polyhedra structure and even honeycomb structures with an increase in the concentration and molecular weight of t-BDDA macro-cross-linker. The use of t-BDDA macro-cross-linker strengthened the molecular chains and resulted in higher tensile properties. As a result, the nanostructured polymer films synthesized from the biphasic polymer latex are expected to find great applicability in the fortification of flexible latex films and the introduction of advanced functional moieties into the whole film.

Acknowledgement This work was supported in part by the National Research Laboratory program (project no. 2000-N-01-C-270) of the Ministry of Science and Technology, South Korea.

References

1. Winnik MA (1997) In: Lovell PA, El-Aasser MS (eds) Emulsion polymerization and emulsion polymers. Wiley, New York, pp 467–518
2. Provder T, Winnik MA, Urban MW (1996) Film formation in waterborne coatings. ACS symposium series 648. American Chemical Society, Washington, DC
3. Perez E, Lang J (1996) Langmuir 12:3180
4. Perez E, Lang J (1999) Macromolecules 32:1626
5. Butt H, Kuropka J, Christensen R (1994) Colloid Polym Sci 272:1218
6. Goudy, Gee ML, Gerharz B (1995) Langmuir 11:4454
7. Hahn K, Ley G, Oberthur R (1998) Colloid Polym Sci 266:631
8. Tamai T, Pineng P, Winnik MA (1999) Macromolecules 32:6102
9. Roulstone BJ, Wilkinson MC, Hearn J (1992) Polym Int 27:43
10. (a) Kawaguchi S, Odrobina E, Winnik MA (1995) Macromol Rapid Commun 16:861; (b) Odrobina E, Feng J, Kawaguchi S, Winnik MA, Neag M, Meyer EF (1998) Macromolecules 31:7239; (c) Tamai T, Pineng P, Winnik MA (1999) Macromolecules 32:6102
11. Chevalier Y, Pichot C, Grailat C, Joanicot M, Wong K, Maquet J, Lindner P, Cabane B (1992) Colloid Polym Sci 270:807
12. Kim HB, Wang Y, Winnik MA (1994) Polymer 35:1779
13. Juhue D, Lang J (1995) Macromolecules 28:1306
14. Sommer F, Duc TM, Pirri R, Meunier G, Quet C (1995) Langmuir 11:440
15. (a) Kim JW, Suh KD (2000) Polymer 41:6181; (b) Kim JW, Ko JY, Suh KD (2001) Macromol Rapid Commun 22:257
16. (a) Mortensen K, Brown W, Jorgensen E (1995) Macromolecules 28:1458; (b) Mortensen K (1997) Macromolecules 30:503
17. Farinha JPS, Martinho JMG (1996) J Phys Chem 100:12552
18. Ho CC, Khew MC (1999) Langmuir 15:6208